

Normalized Wasserstein Distance for Mixture Distributions with Applications in Adversarial Learning and Domain Adaptation

Yogesh Balaji^{1,2} Rama Chellappa^{2,3} Soheil Feizi^{1,2}

Abstract

Understanding proper distance measures between distributions is at the core of several learning tasks such as generative models, domain adaptation, clustering, etc. In this work, we focus on *mixture distributions* that arise naturally in several application domains where the data contains different sub-populations. For mixture distributions, established distance measures such as the Wasserstein distance do not take into account imbalanced mixture proportions. Thus, even if two mixture distributions have identical mixture components but different mixture proportions, the Wasserstein distance between them will be large. This often leads to undesired results in distance-based learning methods for mixture distributions. In this paper, we resolve this issue by introducing *Normalized Wasserstein* distance. The key idea is to introduce mixture proportions as optimization variables, effectively normalizing mixture proportions in the Wasserstein formulation. Using the proposed normalized Wasserstein distance, instead of the vanilla one, leads to significant gains working with mixture distributions with imbalanced mixture proportions. We demonstrate effectiveness of the proposed distance in GANs, domain adaptation, adversarial clustering and hypothesis testing over mixture of Gaussians, MNIST, CIFAR-10, CelebA and VISDA datasets.

1. Introduction

Quantifying distances between probability distributions is a fundamental problem in machine learning and statistics with several applications in generative models, domain adapta-

¹Computer Science Department, University of Maryland, College Park. ²University of Maryland Institute for Advanced Computer Studies. ³Electrical and Computer Engineering Department, University of Maryland, College Park.. Correspondence to: Yogesh Balaji <yogesh@cs.umd.edu>, Soheil Feizi <sfeizi@cs.umd.edu>.

tion, hypothesis testing, etc. Popular probability distance measures include *optimal transport* measures such as the Wasserstein distance (Villani, 2008) and *divergence* measures such as the Kullback-Leibler (KL) divergence (Cover & Thomas, 2012).

Classical distance measures, however, can lead to some issues for mixture distributions. A *mixture distribution* is the probability distribution of a random variable X where $X = X_i$ with probability π_i for $1 \leq i \leq k$. k is the number of mixture components and $\pi = [\pi_1, \dots, \pi_k]^T$ is the vector of *mixture (or mode) proportions*. The probability distribution of each X_i is referred to as a *mixture component* (or, a mode). Mixture distributions arise naturally in different applications where the data contains two or more sub-populations. For example, image datasets with different labels can be viewed as mixture (or, multi-modal) distributions where samples with the same label characterize a specific mixture component. Another prominent example is the *Mixture of Gaussians* (MoG) where every mixture component has a Gaussian distribution.

If two mixture distributions have exactly same mixture components (i.e. same X_i 's) with different mixture proportions (i.e. different π 's), classical distance measures between the two will be large. This can lead to undesired results in several distance-based machine learning methods. To illustrate this issue, consider the *Wasserstein distance* between two distributions \mathbb{P}_X and \mathbb{P}_Y , defined as (Villani, 2008)

$$W(\mathbb{P}_X, \mathbb{P}_Y) := \min_{\mathbb{P}_{X,Y}} \mathbb{E} [\|X - Y\|], \quad (1)$$

$$\text{marginal}_X(\mathbb{P}_{X,Y}) = \mathbb{P}_X, \quad \text{marginal}_Y(\mathbb{P}_{X,Y}) = \mathbb{P}_Y$$

where $\mathbb{P}_{X,Y}$ is the joint distribution (or coupling) whose marginal distributions are equal to \mathbb{P}_X and \mathbb{P}_Y . When no confusion arises and to simplify notation, in some equations, we use $W(X, Y)$ notation instead of $W(\mathbb{P}_X, \mathbb{P}_Y)$.

The Wasserstein distance optimization is over all joint distributions (couplings) $\mathbb{P}_{X,Y}$ whose marginal distributions *match* exactly with input distributions \mathbb{P}_X and \mathbb{P}_Y . This requirement can cause issues when \mathbb{P}_X and \mathbb{P}_Y are mixture distributions with different mixture proportions. In this case, due to the marginal constraints, samples belonging to very different mixture components will have to be coupled to

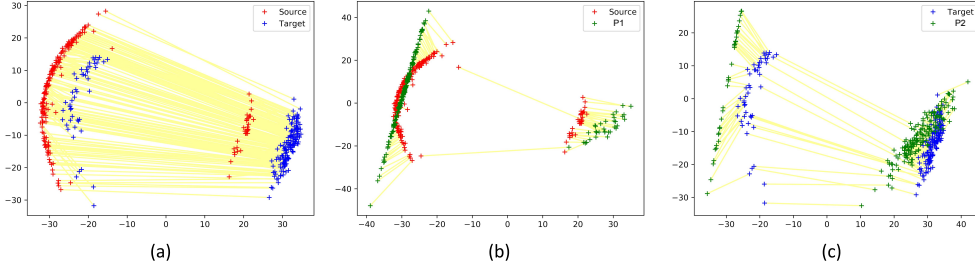


Figure 1. An illustration of the effectiveness of the proposed Normalized Wasserstein distance in domain adaptation. The source domain (shown in red) and the target domain (shown in blue) have two modes with different mode proportions. (a) The couplings computed by estimating Wasserstein distance between source and target distributions (shown with yellow lines) match several samples from incorrect and far mode components. (b,c) Our proposed normalized Wasserstein distance (3) constructs intermediate mixture distributions \mathbb{P}_1 and \mathbb{P}_2 (shown in green) with similar mixture components to the source and the target distributions, respectively, but with optimized mixture proportions. This significantly reduces the number of couplings between samples from incorrect modes and leads to 42% decrease in target loss in domain adaptation compared to the baseline.

gether in $\mathbb{P}_{X,Y}$ (e.g. Figure 1(a)). Thus, using this distance measure can then lead to undesirable outcomes in problems such as domain adaptation. This motivates the need for developing a new distance measure to take into account mode imbalances in mixture distributions.

In this paper, we propose a new distance measure that resolves the issue of imbalanced mixture proportions for multimodal distributions. Our developments focus on a class of optimal transport measures, namely the Wasserstein distance Eq (1). However, our ideas can be extended naturally to other distance measures (eg. adversarial distances (Ganin & Lempitsky, 2015)) as well.

Let \mathbf{G} be an array of generator functions with k components defined as $\mathbf{G} := [\mathbf{G}_1, \dots, \mathbf{G}_k]$. Let $\mathbb{P}_{\mathbf{G},\pi}$ be a mixture probability distribution for a random variable X where $X = \mathbf{G}_i(Z)$ with probability π_i for $1 \leq i \leq k$. Throughout the paper, we assume that Z has a normal distribution.

By relaxing marginal constraints of the classical Wasserstein distance (1), we introduce the *Normalized Wasserstein distance (NW distance)* as follows:

$$\begin{aligned} \tilde{W}(\mathbb{P}_X, \mathbb{P}_Y) \\ := \min_{\mathbf{G}, \pi^{(1)}, \pi^{(2)}} W(\mathbb{P}_X, \mathbb{P}_{\mathbf{G}, \pi^{(1)}}) + W(\mathbb{P}_Y, \mathbb{P}_{\mathbf{G}, \pi^{(2)}}). \end{aligned}$$

There are two key ideas in this definition that help resolve mode imbalance issues for mixture distributions. First, instead of directly measuring the Wasserstein distance between \mathbb{P}_X and \mathbb{P}_Y , we construct two intermediate (and potentially mixture) distributions, namely $\mathbb{P}_{\mathbf{G}, \pi^{(1)}}$ and $\mathbb{P}_{\mathbf{G}, \pi^{(2)}}$. These two distributions have the same mixture components (i.e. same \mathbf{G}) but can have different mixture proportions (i.e. $\pi^{(1)}$ and $\pi^{(2)}$ can be different). Second, mixture proportions, $\pi^{(1)}$ and $\pi^{(2)}$, are considered as optimization variables. This effectively *normalizes* mixture proportions before Wasserstein distance computations. See an example in Figure 1

(b, c) for a visualization of $\mathbb{P}_{\mathbf{G}, \pi^{(1)}}$ and $\mathbb{P}_{\mathbf{G}, \pi^{(2)}}$, and the re-normalization step.

In this paper, we show the effectiveness of the proposed Normalized Wasserstein distance in four application domains. In each case, the performance of our proposed method significantly improves against baselines when input datasets are mixture distributions with imbalanced mixture proportions. Below, we briefly highlight these results:

GANs: In Section 3, we use the normalized Wasserstein distance in GAN's formulation to train mixture models with varying mode proportions. We show that such a generative model can help capture rare modes, decrease the complexity of the generator, and re-normalize an imbalanced dataset.

Domain Adaptation: In Section 4, we formulate the problem of domain adaptation by minimizing the normalized Wasserstein distance between source and target feature embeddings. On classification tasks with imbalanced datasets, our method significantly outperforms baselines (e.g. $\sim 10\%$ accuracy gain in MNIST \rightarrow MNIST-M adaptation, and $\sim 20\%$ gain in synthetic to real adaptation on VISDA-3 dataset). On the unsupervised image-denoising task, our method improves the baseline by 42%.

Adversarial Clustering: In Section 5, we formulate the clustering problem as an adversarial learning task. First, we train a generative mixture model over input data using the proposed normalized Wasserstein distance. Then, we assign each sample to a generative component (cluster) using a minimum distance optimization. We observe that our method obtains high quality clusters on an imbalanced MNIST-3 dataset, and significantly improves over the baselines.

Hypothesis Testing: In Section 6, we propose a test using a combination of Wasserstein and normalized Wasserstein distances to identify if two mixture distributions differ in mode

components or mode proportions. Such a test can provide better understanding while comparing mixture distributions.

2. Normalized Wasserstein Distance

In this section, we introduce the *normalized Wasserstein* distance and discuss its properties. Recall that \mathbf{G} is an array of generator functions defined as $\mathbf{G} := [\mathbf{G}_1, \dots, \mathbf{G}_k]$ where $\mathbf{G}_i : \mathbb{R}^r \rightarrow \mathbb{R}^d$. Let \mathcal{G} be the set of all possible \mathbf{G} function arrays. Let π be a discrete probability mass function with k elements, i.e. $\pi = [\pi_1, \pi_2, \dots, \pi_k]$ where $\pi_i \geq 0$ and $\sum_i \pi_i = 1$. Let Π be the set of all possible π 's.

Let $\mathbb{P}_{\mathbf{G}, \pi}$ be a mixture probability distribution, i.e. it is the probability distribution of a random variable X such that $X = \mathbf{G}_i(Z)$ with probability π_i for $1 \leq i \leq k$. We assume that Z has a normal distribution, i.e. $Z \sim \mathcal{N}(\mathbf{0}, \mathbf{I})$. We refer to \mathbf{G} and π as mixture components and proportions, respectively. The set of all such mixture distributions is defined as follows:

$$\mathcal{P}_{\mathbf{G}, k} := \{\mathbb{P}_{\mathbf{G}, \pi} : \mathbf{G} \in \mathcal{G}, \pi \in \Pi\} \quad (2)$$

where k is the number of mixture components. This set captures a rich family of probability distributions. Given two distributions \mathbb{P}_X and \mathbb{P}_Y belonging to the family of mixture distributions $\mathcal{P}_{\mathbf{G}, k}$, we are interested in defining a distance measure agnostic to differences in mode proportions, but sensitive to shifts in mode components, i.e., the distance function should have high values only when mode components of \mathbb{P}_X and \mathbb{P}_Y differ. If \mathbb{P}_X and \mathbb{P}_Y have the same mode components but differ only in mode proportions, the distance should be low.

The main idea is to introduce mixture proportions as optimization variables in the Wasserstein distance formulation (1). This leads to the following distance measure which we refer to as the *Normalized Wasserstein distance* (NW distance), $\tilde{W}(\mathbb{P}_X, \mathbb{P}_Y)$, defined as:

$$\begin{aligned} \min_{\mathbf{G}, \pi^{(1)}, \pi^{(2)}} \quad & W(\mathbb{P}_X, \mathbb{P}_{\mathbf{G}, \pi^{(1)}}) + W(\mathbb{P}_Y, \mathbb{P}_{\mathbf{G}, \pi^{(2)}}) \quad (3) \\ \text{subject to} \quad & \sum_{j=1}^k \pi_j^{(i)} = 1 \quad i = 1, 2, \\ & \pi_j^{(i)} \geq 0 \quad 1 \leq j \leq k, \quad i = 1, 2. \end{aligned}$$

Since the normalized Wasserstein's optimization (3) includes mixture proportions $\pi^{(1)}$ and $\pi^{(2)}$ as optimization variables, if two mixture distributions have similar mixture components with different mixture proportions (i.e. $\mathbb{P}_X = \mathbb{P}_{\mathbf{G}, \pi^{(1)}}$ and $\mathbb{P}_Y = \mathbb{P}_{\mathbf{G}, \pi^{(2)}}$), although the Wasserstein distance between the two can be large, the introduced normalized Wasserstein distance between the two will be zero. Note that \tilde{W} is defined with respect to a set of generator functions $\mathbf{G} = [\mathbf{G}_1, \dots, \mathbf{G}_k]$. However, to simplify the notation, we make this dependency implicit.

To compute the NW distance, we use an alternating gradient decent approach similar to the dual computation of the Wasserstein distance (Arjovsky et al., 2017). Moreover, we impose the π constraints using a soft-max function. For details, see Section 2 of Supplementary material.

To illustrate how NW distance is agnostic to mode imbalances between distributions, consider an unsupervised *domain adaptation* problem with MNIST-2 (i.e. a dataset with two classes: digits 1 and 2 from MNIST) as the source dataset, and noisy MNIST-2 (i.e. a noisy version of it) as the target dataset (details of this example is presented in Section 4.2). The source dataset has 4/5 digits one and 1/5 digits two, while the target dataset has 1/5 noisy digits one and 4/5 noisy digits two. The couplings produced by estimating Wasserstein distance between the two distributions is shown in yellow lines in Figure 1-a. We observe that there are many couplings between samples from incorrect mixture components. The normalized Wasserstein distance, on the other hand, constructs intermediate mode-normalized distributions \mathbb{P}_1 and \mathbb{P}_2 , which get coupled to the correct modes of source and target distributions, respectively (see panels (b) and (c) in Figure 1)).

In what follows, we demonstrate applications of the introduced normalized Wasserstein distance in four machine learning problems - generative models, domain adaptation, hypothesis testing and adversarial clustering for mixture distributions.

3. Normalized Wasserstein GAN

Learning a probability model from data is a fundamental problem in statistics and machine learning. Building on the success of deep learning, a recent approach to this problem is using Generative Adversarial Networks (GANs) (Goodfellow et al., 2014). GANs view this problem as a *game* between a *generator* whose goal is to generate fake samples that are close to the real data training samples, and a *discriminator* whose goal is to distinguish between the real and fake samples. The generator and the discriminator functions are typically implemented as deep neural networks.

Most GAN frameworks can be viewed as methods that *minimize* a distance between the observed probability distribution, \mathbb{P}_X , and the generative probability distribution, \mathbb{P}_Y , where $Y = \mathbf{G}(Z)$. \mathbf{G} is referred to as the generator function. In several GAN formulations, the *distance* between \mathbb{P}_X and \mathbb{P}_Y is formulated as another optimization which characterizes the discriminator. Several GAN architectures have been proposed in the last couple of years. A summarized list includes GANs based on **optimal transport** measures (e.g. Wasserstein GAN+Weight Clipping (Arjovsky et al., 2017), WGAN+Gradient Penalty (Gulrajani et al., 2017), GAN+Spectral Normalization (Miyato et al.,

2018), WGAN+Truncated Gradient Penalty (Petzka et al., 2017), relaxed WGAN (Guo et al., 2017)), GANs based on **divergence** measures (e.g. the original GAN’s formulation (Goodfellow et al., 2014), DCGAN (Radford et al., 2015), f -GAN (Nowozin et al., 2016)), GANs based on **moment-matching** (e.g. MMD-GAN (Dziugaite et al., 2015; Li et al., 2015)), and other formulations (e.g. Least-Squares GAN (Mao et al., 2016), Boundary equilibrium GAN (Berthelot et al., 2017), BigGAN (Brock et al., 2018), etc.)

If the observed distribution \mathbb{P}_X is a mixture one, the proposed normalized Wasserstein distance (3) can be used to compute a generative model. Instead of estimating a single generator \mathbf{G} as done in standard GANs, we estimate a mixture distribution $\mathbb{P}_{\mathbf{G}, \pi}$ using the proposed NW distance. We refer to this GAN as the *Normalized Wasserstein GAN* (or NWGAN) formulated as the following optimization:

$$\min_{\mathbf{G}, \pi} \tilde{W}(\mathbb{P}_X, \mathbb{P}_{\mathbf{G}, \pi}). \quad (4)$$

In this case, the NW distance simplifies as

$$\begin{aligned} & \min_{\mathbf{G}, \pi} \tilde{W}(\mathbb{P}_X, \mathbb{P}_{\mathbf{G}, \pi}) \\ &= \min_{\mathbf{G}, \pi} \min_{\mathbf{G}', \pi^{(1)}, \pi^{(2)}} W(\mathbb{P}_X, \mathbb{P}_{\mathbf{G}', \pi^{(1)}}) + W(\mathbb{P}_{\mathbf{G}, \pi}, \mathbb{P}_{\mathbf{G}', \pi^{(2)}}) \\ &= \min_{\mathbf{G}, \pi} W(\mathbb{P}_X, \mathbb{P}_{\mathbf{G}, \pi}). \end{aligned} \quad (5)$$

There are couple of differences between the proposed NWGAN and the existing GAN architectures. The generator in the proposed NWGAN is a mixture of k models, each producing π_i fraction of generated samples. We select k a priori based on the application domain while π is computed within the NW distance optimization. Modeling the generator as a mixture of k neural networks have also been investigated in some recent works (Hoang et al., 2018; Ghosh et al., 2017). However, these methods assume that the mixture proportions π are known beforehand, and are held fixed during the training. In contrast, our approach is more general as the mixture proportions are also optimized. Estimating mode proportions have several important advantages: (1) we can estimate rare modes, (2) an imbalanced dataset can be re-normalized, (3) by allowing each \mathbf{G}_i to focus only on one part of the distribution, the quality of the generative model can be improved while the complexity of the generator can be reduced. In the following, we highlight these properties of NWGAN on different datasets.

3.1. Mixture of Gaussians

First, we illustrate results of training NWGAN on a two dimensional mixture of Gaussians. The input data is a mixture of 9 Gaussians, each centered at a vertex of a 3×3 grid as shown in Figure 2. The mean and the covariance matrix for each mode are randomly chosen. The mode proportion

for mode i is chosen as $\pi_i = \frac{i}{45}$ for $1 \leq i \leq 9$ (note that $\sum_i \pi_i = 1$).

Generations produced by NWGAN using $k = 9$ affine generator models on this dataset is shown in Figure 2. We also compare our method with the vanilla WGAN (Arjovsky et al., 2017) and MGAN (Hoang et al., 2018). Since MGAN does not optimize over π , we assume uniform mode proportions ($\pi_i = 1/9$ for all i). To train vanilla WGAN, a non-linear generator function is used since a single affine function cannot model a mixture of Gaussian distribution.

To evaluate the generative models, we report the following quantitative scores: (1) the average mean error which is the mean-squared error (MSE) between the mean vectors of real and generated samples per mode averaged over all modes, (2) the average covariance error which is the MSE between the covariance matrices of real and generated samples per mode averaged over all modes, and (3) the π estimation error which is the normalized MSE between the π vector of real and generated samples. Note that computing these metrics require mode assignments for generated samples. This is done based on the closeness of generative samples to the ground-truth means.

We report these error terms for different GANs in Table 1. We observe that the proposed NWGAN achieves best scores compared to the other two approaches. Also, from Figure 2, we observe that the generative model trained by MGAN misses some of the rare modes in the data. This is because of the error induced by assuming fixed mixture proportions when the ground-truth π is non-uniform. Since our proposed NWGAN estimates π in the optimization, even rare modes in the data are not missed. This shows the importance of estimating mixture proportions specially when the input dataset has imbalanced modes.

Table 1. Quantitative Evaluation on Mixture of Gaussians

Method	Avg. μ error	Avg. Σ error	π error
WGAN	0.007	0.0003	0.0036
MGAN	0.007	0.0002	0.7157
NWGAN	0.002	0.0001	0.0001

3.2. A Mixture of CIFAR-10 and CelebA

One benefit of learning mixture generative models is to disentangle the data distribution into multiple components where each component represents one mode of the input distribution. Such disentanglement is useful in many tasks such as clustering as we discuss in Section 5. To test the effectiveness of NWGAN in performing such disentanglement, we consider a mixture of 50,000 images from CIFAR-10 and 100,000 images from CelebA (Liu et al., 2015) datasets as our input distribution. All images are reshaped to be

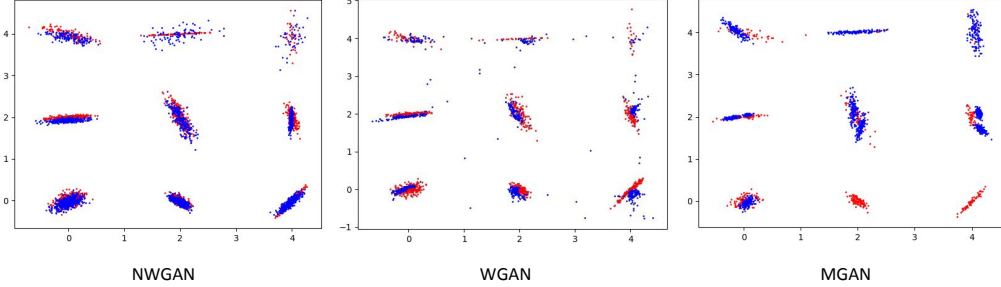


Figure 2. Mixture of Gaussian experiments. In all figures, red points indicate samples from the real data distribution while blue points indicate samples from the generated distribution. NWGAN is able to capture rare modes in the data and produces a significantly better generative model than other methods.

32×32 .

To highlight the importance of optimizing mixture proportion to produce disentangled generative models, we compare the performance of NWGAN with a variation of NWGAN where the mode proportion π is held fixed as $\pi_i = \frac{1}{k}$ (the uniform distribution). Sample generations produced by both models are shown in Figure 3. When π is held fixed, the model does not produce disentangled representations (in the second mode, we observe a mix of CIFAR and CelebA generative images.) However, when we optimize π , each generator produces distinct modes.

4. Normalized Wasserstein in Domain Adaptation

In this section, we demonstrate the effectiveness of the NW distance in Unsupervised Domain Adaptation (UDA) both for supervised (e.g. classification) and unsupervised (e.g. denoising) tasks. Note that the term *unsupervised* in UDA means that the label information in the target domain is unknown while *unsupervised* tasks mean that the label information in the source domain is unknown.

First, we consider domain adaptation for a classification task. Let (X_s, Y_s) represent the source domain while (X_t, Y_t) denote the target domain. Since we deal with the classification setup, we have $Y_s, Y_t \in \{1, 2, \dots, k\}$. A common formulation for the domain adaptation problem is to transform X_s and X_t to a feature space where the *distance* between the source and target feature distributions is sufficiently small, while a good classifier can be computed for the source domain in that space (Ganin & Lempitsky, 2015). In this case, one solves the following optimization:

$$\min_{f \in \mathcal{F}} L_{cl}(f(X_s), Y_s) + \lambda \text{dist}(f(X_s), f(X_t)) \quad (6)$$

where λ is an adaptation parameter and L_{cl} is the empirical classification loss function (e.g. the cross-entropy loss). The distance function between distributions can be adversarial

distances (Ganin & Lempitsky, 2015; Tzeng et al., 2017), the Wasserstein distance (Shen et al., 2018), or MMD-based distances (Long et al., 2015; 2016).

When X_s and X_t are mixture distributions (which is often the case as each label corresponds to one mixture component) with different mixture proportions, the use of these classical distance measures can lead to computation of inappropriate transformation and classification functions. In this case, we propose to use the NW distance as follows:

$$\min_{f \in \mathcal{F}} L_{cl}(X_s, Y_s) + \lambda \tilde{W}(f(X_s), f(X_t)). \quad (7)$$

Computing the NW distance requires training mixture components \mathbf{G} and mode proportions $\pi^{(1)}, \pi^{(2)}$. To simplify the computation, we make use of the fact that labels for the source domain (i.e. Y_s) are known, thus source mixture components can be identified using these labels. Using this information, we can avoid the need for computing \mathbf{G} directly and use the conditional source feature distributions as a proxy for the mixture components as follows:

$$\begin{aligned} \mathbf{G}_i(Z) &\stackrel{\text{dist}}{=} f(X_s^{(i)}), \\ X_s^{(i)} &= \{X_s | Y_s = i\}, \quad \forall 1 \leq i \leq k, \end{aligned} \quad (8)$$

where $\stackrel{\text{dist}}{=}$ means matching distributions. Using (8), the formulation (7) can be simplified as

$$\min_{f \in \mathcal{F}} \min_{\pi} L_{cl}(X_s, Y_s) + \lambda W \left(\sum_i \pi^{(i)} f(X_s^{(i)}), f(X_t) \right). \quad (9)$$

The above formulation can be seen as a version of instance weighting as source samples in $X_s^{(i)}$ are weighted by π_i . Instance weighting mechanisms have been well studied for domain adaptation (Yan et al., 2017; Yu & Szepesvári, 2012). However, different to these approaches, we train the mode proportion vector π in an end-to-end fashion using neural networks and integrate the instance weighting in a Wasserstein optimization. Of more relevance to our work is the



Figure 3. Sample generations of NWGAN with $k = 2$ on a mixture of CIFAR-10 and CelebA datasets for fixed and optimized π 's. When π is fixed, one of the generators produces a mix of CIFAR and CelebA generative images (boxes in red highlight some of the CelebA generations in the model producing CIFAR+CelebA). However, when π is optimized, the model produces disentangled representations.

method proposed in (Chen et al., 2018), where the instance weighting is trained end-to-end in a neural network. However, in (Chen et al., 2018), instance weights are maximization variable with respect to the Wasserstein loss, while we show that the mixture proportions need to minimization variables to normalize mode mismatches. Moreover, our NW distance formulation can handle the case when mode assignments for source embeddings are unknown (as we discuss in Section 4.2). This case cannot be handled by the formulation of (Chen et al., 2018).

For unsupervised tasks when mode assignments for source samples are unknown, we cannot use the simplified formulation of (8). In that case, we use a domain adaptation method solving the following optimization:

$$\min_{f \in \mathcal{F}} L_{unsup}(X_s) + \lambda \tilde{W}(f(X_s), f(X_t)), \quad (10)$$

where $L_{unsup}(X_s)$ is the loss corresponding to the desired *unsupervised* learning task on the source domain data.

4.1. UDA for supervised tasks

In this section, we present experiments on a domain adaptation problem for a classification task with imbalanced source and target domain datasets.

4.1.1. MNIST \rightarrow MNIST-M

In the first set of experiments, we consider adaptation between MNIST \rightarrow MNIST-M datasets, one of the benchmark tasks for the domain adaptation problem. We consider three settings with imbalanced class proportions in source and target datasets: 3 modes, 5 modes, and 10 modes. More details can be found in Table 7 of the Supplementary material.

Following (Ganin & Lempitsky, 2015), we use a modified Lenet architecture for the feature network, and a two-layer MLP for the domain discriminator. We compare our method with the following approaches: (1) Source-only which is a baseline model trained only on source domain with no

domain adaptation performed, (2) DANN (Ganin & Lempitsky, 2015), a method where adversarial distance between source and target distributions is minimized, and (3) Wasserstein (Shen et al., 2018) where Wasserstein distance between source and target distributions is minimized. Table 2 summarizes our results of this experiment. We observe that performing domain adaptation using adversarial distance and Wasserstein distance leads to decrease in performance compared to the baseline model. This is partially owing to not accounting for mode imbalances, thus resulting in negative transfer, i.e., samples belonging to incorrect classes are coupled and getting pushed to be close in the embedding. Our proposed NW distance, however, accounts for mode imbalances and leads to a significant boost in performance in all three settings.

Table 2. Mean classification accuracies (in %) averaged over 5 runs on MNIST \rightarrow MNIST-M adaptation

Method	3 modes	5 modes	10 modes
Source only	66.63	67.44	63.17
DANN	62.34	57.56	59.31
Wasserstein	61.75	60.56	58.22
NW distance	75.06	76.16	68.57

4.1.2. VISDA

In the experiment of Section 4.1.1 on digits dataset, models have been trained from scratch. However, a common practice used in domain adaptation is to transfer knowledge from a pretrained network (eg. models trained on ImageNet) and fine-tune on the desired task. To evaluate the performance of our approach in such settings, we consider adaptation on the VISDA dataset (Peng et al., 2017); a recently proposed benchmark for adapting from synthetic to real images.

We consider a subset of the entire VISDA dataset containing the following three classes: *aeroplane*, *horse* and *truck*. The source domain contains (0.55, 0.33, 0.12) fraction of samples per class, while that of the target domain

is $(0.12, 0.33, 0.55)$. We use a Resnet-18 model pre-trained on ImageNet as our feature network. As shown in Table 3, our approach significantly improves the domain adaptation performance over the baseline and other compared methods.

Table 3. Mean classification accuracies (in %) averaged over 5 runs on synthetic to real adaptation on VISDA dataset (3 classes)

Method	Accuracy (in %)
Source only	53.19
DANN	68.06
Wasserstein	64.84
Normalized Wasserstein	73.23

4.2. UDA for unsupervised tasks

For unsupervised tasks on mixture datasets, we use the formulation of Eq (10) to perform domain adaptation. To empirically validate this formulation, we consider the image denoising problem. The source domain consists of digits $\{1, 2\}$ from MNIST dataset as shown in Fig 4(a). Note that the color of digit 2 is inverted. The target domain is a noisy version of the source, i.e. source images are perturbed with random *i.i.d* Gaussian noise $\mathcal{N}(0.4, 0.7)$ to obtain target images. Our dataset contains 5,000 samples of digit 1 and 1,000 samples of digit 2 in the source domain, and 1,000 samples of noisy digit 1 and 5,000 samples of noisy digit 2 in the target. The task is to perform image denoising by dimensionaly reduction, i.e., given a target domain image, we need to reconstruct the corresponding clean image that looks like the source. We assume that no (source, target) correspondence is available in the dataset.

To perform denoising when the (source, target) correspondence is unavailable, a natural choice would be to minimize the reconstruction loss in the source domain while minimizing the distance between source and target embedding distributions. We use the NW distance as our choice of distance measure. This results in the following optimization:

$$\min_{f,g} \mathbb{E}_{\mathbf{x} \sim X_s} \|g(f(\mathbf{x})) - \mathbf{x}\|_2^2 + \lambda \tilde{W}(f(X_s), f(X_t))$$

where $f(\cdot)$ is the encoder and $g(\cdot)$ is the decoder.

As our baseline, we consider a model trained only on source using a quadratic reconstruction loss. Fig 4(b) shows source and target embeddings produced by this baseline. In this case, the source and the target embeddings are distant from each other. However, as shown in Fig 4(c), using the NW distance formulation, the distributions of source and target embeddings match closely (with estimated mode proportions). We measure the L_2 reconstruction loss of the target domain, $err_{recons,tgt} = \mathbb{E}_{\mathbf{x} \sim X_t} \|g(f(\mathbf{x})) - \mathbf{x}\|_2^2$, as a quantitative evaluation measure. This value for different approaches is shown in Table 4. We observe that our method outperforms the compared approaches.

Table 4. $err_{recons,tgt}$ for an image denoising task

Method	$err_{recons,tgt}$
Source only	0.31
Wasserstein	0.52
Normalized Wasserstein	0.18
Training on target (Oracle)	0.08

5. Adversarial Clustering

In this section, we use the proposed NW distance to formulate an adversarial clustering approach. More specifically, let the input data distribution have k underlying modes (each representing a cluster), which we intend to recover. The use of generative models for clustering has been explored in some of the recent works. In (Locatello et al., 2018), VAEs are used to perform clustering. Clustering using GANs is performed in (Yu & Zhou, 2018) using an Expectation-Maximization approach. Different from these, our approach makes use of the proposed NWGAN for clustering, and thus can explicitly handle data with imbalanced modes.

Let \mathbb{P}_X be observed empirical distribution. Let \mathbf{G}^* and π^* be optimal solutions of NWGAN optimization (5). For a given point $\mathbf{x}_i \sim \mathbb{P}_X$, the clustering assignment is computed using the closest distance to a mode. I.e.,

$$C(\mathbf{x}_i) = \arg \min_{1 \leq j \leq k} \min_Z [\|\mathbf{x}_i - \mathbf{G}_j(Z)\|^2]. \quad (11)$$

To perform an effective clustering, we require each mode \mathbf{G}_j to capture one mode of the data distribution. Without enforcing any regularization and using rich generator functions, one model can capture multiple modes of the data distribution. To prevent this, we introduce a *regularization* term that maximizes the weighted average Wasserstein distances between different generated modes. That is,

$$R = \sum_{(i,j)|i>j} \pi_i \pi_j W(\mathbf{G}_i(Z), \mathbf{G}_j(Z)).$$

This term encourages *diversity* among generative modes. With this regularization term, the optimization objective of a *regularized* NWGAN becomes

$$\min_{\mathbf{G}, \pi} W(\mathbb{P}_X, \mathbb{P}_{\mathbf{G}, \pi}) - \lambda_{reg} R$$

where λ_{reg} is the regularization parameter.

We test the proposed adversarial clustering on an imbalanced MNIST dataset with 3 digits containing 3,000 samples of digit 2, 1,500 samples of digit 4 and 6,000 samples of digit 6. We compare our approach with *k-means* clustering and *Gaussian Mixture Model (GMM)*. Cluster purity, NMI and ARI scores are used as quantitative metrics (refer to Appendix Section C.3 for more details). Performance of our approach in comparison with the other two techniques is shown in Table 5. Our clustering technique is able to achieve good performance than the other two methods.

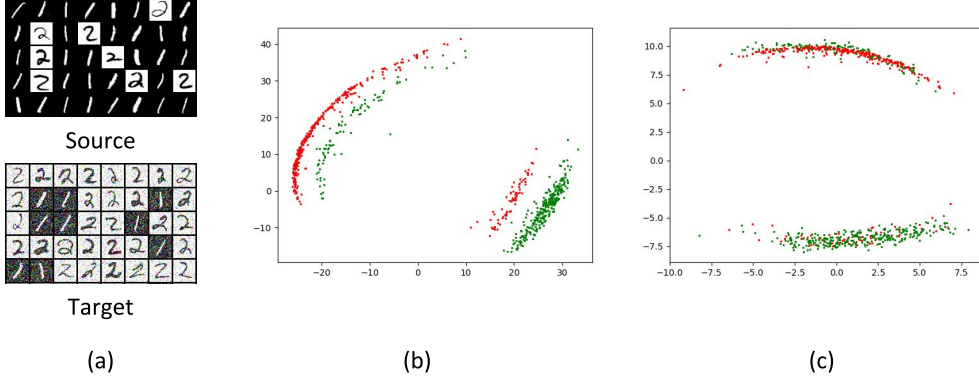


Figure 4. Domain adaptation for image denoising. (a) Samples from source and target domains. (b) Source and target embeddings learnt by the baseline model. (c) Source and target embeddings learnt by minimizing the proposed NW distance. In (b) and (c), red and green points indicate source and target samples, respectively.

Table 5. Clustering results on Imbalanced MNIST dataset

Method	Cluster Purity	NMI	ARI
k-means	0.82	0.49	0.43
GMM	0.75	0.28	0.33
NW distance	0.98	0.94	0.97

6. Hypothesis Testing

Suppose \mathbb{P}_X and \mathbb{P}_Y are two mixture distributions with the same mixture components but different mode proportions. I.e., \mathbb{P}_X and \mathbb{P}_Y both belong to $\mathcal{P}_{G,k}$. In this case, depending on the difference between $\pi^{(1)}$ and $\pi^{(2)}$, the Wasserstein distance between the two distributions can be arbitrarily large. Thus, using the Wasserstein distance, we can only conclude that the two distributions are different. In some applications, it can be informative to have a test that determines if two distributions differ only in mode proportions. We propose a test based on a combination of Wasserstein and the NW distance for this task. This procedure is shown in Table 6. We note that computation of p -values for the proposed test is beyond the scope of this paper.

Table 6. Hypothesis test between two mixture distributions

Wasserstein distance	NW distance	Conclusion
High	High	Distributions differ in mode components
High	Low	Distributions have the same components, but differ in mode proportions
Low	Low	Distributions are the same

We demonstrate this test on 2D Mixture of Gaussians. We perform experiments on two settings, each involving two datasets \mathcal{D}_1 and \mathcal{D}_2 , which are mixtures of 8 Gaussians:

Setting 1: Both \mathcal{D}_1 and \mathcal{D}_2 have same mode components, with the i^{th} mode located at $(r \cos(\frac{2\pi i}{8}), r \sin(\frac{2\pi i}{8}))$.

Setting 2: \mathcal{D}_1 and \mathcal{D}_2 have shifted mode components. The i^{th} mode of \mathcal{D}_1 is located at $(r \cos(\frac{2\pi i}{8}), r \sin(\frac{2\pi i}{8}))$, while the i^{th} mode of \mathcal{D}_2 is located at $(r \cos(\frac{2\pi i + \pi}{8}), r \sin(\frac{2\pi i + \pi}{8}))$.

In both the settings, the mode fraction of \mathcal{D}_1 is $\pi_i = \frac{i+2}{52}$, and that of \mathcal{D}_2 is $\pi_i = \frac{11-i}{52}$. We use 2,000 data points from \mathcal{D}_1 and \mathcal{D}_2 to compute Wasserstein and the NW distances in primal form by solving a linear program. The computed distance values are reported in Table 7. In setting 1, we observe that the Wasserstein distance is large while the NW distance is small. Thus, one can conclude that the two distributions differ only in mode proportions. In setting 2, both Wasserstein and NW distances are large. Thus, in this case, distributions differ in mixture components as well.

Table 7. Hypothesis test between two MOG - \mathcal{D}_1 and \mathcal{D}_2

Setting	Wasserstein Distance	NW Distance
Setting 1	1.51	0.06
Setting 2	1.56	0.44

7. Conclusion

In this paper, we first showed that the standard Wasserstein distance, due to its marginal constraints, can lead to undesired results when applied to mixture distributions with imbalanced mixture proportions. To resolve this issue, we proposed a new distance measure called the normalized Wasserstein distance. The key idea is to optimize mixture proportions in the Wasserstein formulation, effectively normalizing mixture imbalance. We demonstrated the usefulness of normalized Wasserstein distance in four machine learning tasks: GANs, domain adaptation, adversarial clustering and hypothesis testing for mixture distributions. Strong empirical results on all four problems highlight the

effectiveness of the proposed distance measure. Normalized Wasserstein distance can be used in other machine learning problems involving distance computation between distributions. Moreover, similar ideas can be extended to other distance measures such as divergence measures as well.

References

Arjovsky, M., Chintala, S., and Bottou, L. Wasserstein GAN. *arXiv preprint arXiv:1701.07875*, 2017.

Berthelot, D., Schumm, T., and Metz, L. BEGAN: boundary equilibrium generative adversarial networks. *arXiv preprint arXiv:1703.10717*, 2017.

Brock, A., Donahue, J., and Simonyan, K. Large scale GAN training for high fidelity natural image synthesis. *CoRR*, abs/1809.11096, 2018.

Chen, Q., Liu, Y., Wang, Z., Wassell, I., and Chetty, K. Re-weighted adversarial adaptation network for unsupervised domain adaptation. In *The IEEE Conference on Computer Vision and Pattern Recognition (CVPR)*, June 2018.

Cover, T. M. and Thomas, J. A. *Elements of information theory*. John Wiley & Sons, 2012.

Dziugaite, G. K., Roy, D. M., and Ghahramani, Z. Training generative neural networks via maximum mean discrepancy optimization. *arXiv preprint arXiv:1505.03906*, 2015.

Ganin, Y. and Lempitsky, V. Unsupervised domain adaptation by backpropagation. In Bach, F. and Blei, D. (eds.), *Proceedings of the 32nd International Conference on Machine Learning*, volume 37 of *Proceedings of Machine Learning Research*, pp. 1180–1189, Lille, France, 07–09 Jul 2015. PMLR.

Ghosh, A., Kulharia, V., Namboodiri, V. P., Torr, P. H., and Dokania, P. K. Multi-agent diverse generative adversarial networks. *CoRR*, abs/1704.02906, 6:7, 2017.

Goodfellow, I., Pouget-Abadie, J., Mirza, M., Xu, B., Warde-Farley, D., Ozair, S., Courville, A., and Bengio, Y. Generative adversarial nets. In *Advances in neural information processing systems*, pp. 2672–2680, 2014.

Gulrajani, I., Ahmed, F., Arjovsky, M., Dumoulin, V., and Courville, A. Improved training of Wasserstein GANs. *arXiv preprint arXiv:1704.00028*, 2017.

Guo, X., Hong, J., Lin, T., and Yang, N. Relaxed wasserstein with applications to GANs. *arXiv preprint arXiv:1705.07164*, 2017.

Hoang, Q., Nguyen, T. D., Le, T., and Phung, D. MGAN: training generative adversarial nets with multiple generators. 2018.

Li, Y., Swersky, K., and Zemel, R. Generative moment matching networks. In *Proceedings of the 32nd International Conference on Machine Learning (ICML-15)*, pp. 1718–1727, 2015.

Liu, Z., Luo, P., Wang, X., and Tang, X. Deep learning face attributes in the wild. In *Proceedings of International Conference on Computer Vision (ICCV)*, 2015.

Locatello, F., Vincent, D., Tolstikhin, I. O., Rätsch, G., Gelly, S., and Schölkopf, B. Clustering meets implicit generative models. *CoRR*, abs/1804.11130, 2018.

Long, M., Cao, Y., Wang, J., and Jordan, M. I. Learning transferable features with deep adaptation networks. In *Proceedings of the 32nd International Conference on Machine Learning*, pp. 97–105, 2015.

Long, M., Wang, J., and Jordan, M. I. Unsupervised domain adaptation with residual transfer networks. *CoRR*, abs/1602.04433, 2016.

Mao, X., Li, Q., Xie, H., Lau, R. Y., and Wang, Z. Multi-class generative adversarial networks with the l2 loss function. *arXiv preprint arXiv:1611.04076*, 2016.

Miyato, T., Kataoka, T., Koyama, M., and Yoshida, Y. Spectral normalization for generative adversarial networks. *arXiv preprint arXiv:1802.05957*, 2018.

Nowozin, S., Cseke, B., and Tomioka, R. f-GAN: training generative neural samplers using variational divergence minimization. In *Advances in Neural Information Processing Systems*, pp. 271–279, 2016.

Peng, X., Usman, B., Kaushik, N., Hoffman, J., Wang, D., and Saenko, K. Visda: The visual domain adaptation challenge. *CoRR*, abs/1710.06924, 2017. URL <http://arxiv.org/abs/1710.06924>.

Petzka, H., Fischer, A., and Lukovnicov, D. On the regularization of Wasserstein GANs. *arXiv preprint arXiv:1709.08894*, 2017.

Radford, A., Metz, L., and Chintala, S. Unsupervised representation learning with deep convolutional generative adversarial networks. *arXiv preprint arXiv:1511.06434*, 2015.

Shen, J., Qu, Y., Zhang, W., and Yu, Y. Wasserstein distance guided representation learning for domain adaptation. In *AAAI*, pp. 4058–4065. AAAI Press, 2018.

Tzeng, E., Hoffman, J., Saenko, K., and Darrell, T. Adversarial discriminative domain adaptation. In *Computer Vision and Pattern Recognition (CVPR)*, volume 1, pp. 4, 2017.

Villani, C. *Optimal transport: old and new*, volume 338. Springer Science & Business Media, 2008.

Yan, H., Ding, Y., Li, P., Wang, Q., Xu, Y., and Zuo, W. Mind the class weight bias: Weighted maximum mean discrepancy for unsupervised domain adaptation. In *2017 IEEE Conference on Computer Vision and Pattern Recognition, CVPR 2017, Honolulu, HI, USA, July 21-26, 2017*, pp. 945–954, 2017.

Yu, Y. and Szepesvári, C. Analysis of kernel mean matching under covariate shift. In *Proceedings of the 29th International Conference on Machine Learning, ICML 2012, Edinburgh, Scotland, UK, June 26 - July 1, 2012*, 2012.

Yu, Y. and Zhou, W.-J. Mixture of gans for clustering. In *Proceedings of the Twenty-Seventh International Joint Conference on Artificial Intelligence, IJCAI-18*, pp. 3047–3053. International Joint Conferences on Artificial Intelligence Organization, 2018.

Appendix

A. Architecture and hyper-parameters

Implementation details including model architectures and hyperparameters are presented in this section:

A.1. Mixture models for Generative Adversarial Networks (GANs)

A.1.1. MIXTURE OF GAUSSIANS

As discussed in Section 3.1 of the main paper, the input dataset is a mixture of 8 Gaussians with varying mode proportion. Normalized Wasserstein GAN was trained with linear generator and non-linear discriminator models using the architectures and hyper-parameters as presented in Table 8. The architecture used for training Vanilla WGAN is provided in Table 9. The same architecture is used for MGAN, however we do not use the *ReLU* non-linearities in the Generator function (to make the generator affine so that the model is comparable to ours). For WGAN and MGAN, we use the hyper-parameter details as provided in the respective papers – (Gulrajani et al., 2017) and (Hoang et al., 2018).

A.1.2. CIFAR-10 + CELEBA

To train models on CIFAR-10 + CelebA dataset (Section 3.2 of the main paper), we used the Resnet architectures of WGAN-GP (Gulrajani et al., 2017) with the same hyper-parameter configuration for the generator and the discriminator networks. In Normalized WGAN, the learning rate of mode proportion π was 5 times the learning rate of the discriminator.

Table 8. Architectures and hyper-parameters: Mixture of Gaussians with Normalized Wasserstein GAN

Generator	Discriminator
Linear(2 → 64)	Linear(2 → 128)
Linear(64 → 64)	LeakyReLU(0.2)
Linear(64 → 64)	Linear(128 → 128)
Linear(64 → 2)	LeakyReLU(0.2)
	Linear(128 → 2)
Hyperparameters	
Discriminator learning rate	0.00005
Generator learning rate	0.00005
π learning rate	0.01
Batch size	1024
Optimizer	RMSProp
Number of critic iters	10
Weight clip	[−0.003, 0.003]

Table 9. Architectures: Mixture of Gaussians with vanilla WGAN model

Generator	Discriminator
Linear(2 → 512) + ReLU	Linear(2 → 512) + ReLU
Linear(512 → 512) + ReLU	Linear(512 → 512) + ReLU
Linear(512 → 512) + ReLU	Linear(512 → 512) + ReLU
Linear(512 → 2)	Linear(512 → 2)

A.2. Domain adaptation for mixture distributions

A.2.1. DIGIT CLASSIFICATION

For MNIST→MNIST-M experiments (Section 4.1.1 of the main paper), following (Ganin & Lempitsky, 2015), a modified Lenet architecture was used for feature network, and a MLP network was used for domain classifier. The architectures and hyper-parameters used in our method are given in Table 10. The same architectures are used for the compared approaches - Source only, DANN and Wasserstein.

A.2.2. VISDA

For the experiments on VISDA dataset with three classes (Section 4.1.2 of the main paper), the architectures and hyper-parameters used in our method are given in Table 11. The same architectures are used for the compared approaches: source only, Wasserstein and DANN.

A.2.3. DOMAIN ADAPTATION FOR IMAGE DENOISING

The architectures and hyper-parameters used in our method for image denoising experiment (Section 4.2 of the main paper) are presented in Table 12. To perform adaptation using Normalized Wasserstein distance, we need to train the intermediate distributions $\mathbb{P}_{G,\pi^{(1)}}$ and $\mathbb{P}_{G,\pi^{(2)}}$ (as discussed in Section 2, 4.2 of the main paper). We denote the generator and discriminator models corresponding to

Table 10. Architectures and hyper-parameters: Domain adaptation for MNIST→MNIST-M experiments

Feature network	
Conv(3 → 32, 5 × 5 kernel)	+ ReLU + MaxPool(2)
Conv(32 → 48, 5 × 5 kernel)	+ ReLU + MaxPool(2)
Domain discriminator	Classifier
Linear(768 → 100) + ReLU	Linear(768 → 100) + ReLU
Linear(100 → 1)	Linear(100 → 100) + ReLU
	Linear(100 → 10)
Hyperparameters	
Feature network learning rate	0.0002
Discriminator learning rate	0.0002
Classifier learning rate	0.0002
π learning rate	0.0005
Batch size	128
Optimizer	Adam
Number of critic iters	10
Weight clipping value	[−0.01, 0.01]
λ	1

Table 11. Architectures and hyper-parameters: Domain adaptation on VISDA dataset

Feature network	
Resnet-18 model pretrained on ImageNet till the penultimate layer	
Domain discriminator	Classifier
Linear(512 → 512) + LeakyReLU(0.2)	Linear(512 → 3)
Linear(512 → 512) + LeakyReLU(0.2)	
Linear(512 → 512) + LeakyReLU(0.2)	
Linear(512 → 1)	
Hyperparameters	
Feature network learning rate	0.000001
Discriminator learning rate	0.00001
Classifier learning rate	0.00001
π learning rate	0.0001
Batch size	128
Optimizer	Adam
Number of critic iters	5
Initial iters	5000
Weight clipping value	[−0.01, 0.01]
λ	1

$\mathbb{P}_{\mathbf{G}, \pi^{(1)}}$ and $\mathbb{P}_{\mathbf{G}, \pi^{(2)}}$ as Generator (RW) and Discriminator (RW) respectively. In practice, we noticed that the Generator (RW) and Discriminator (RW) models need to be trained for a certain number of iterations first (which we call initial iterations) before performing adaptation. So, for these initial iterations, we set the adaptation parameter λ as 0. Note that the encoder, decoder, generator (RW) and discriminator (RW) models are trained during this phase, but the adaptation is not performed. After these initial iterations, we turn the adaptation term on. The hyperparameters and model architectures are given in Table 12. The same architectures are used for Source only and Wasserstein.

Table 12. Architectures and hyper-parameters: Domain adaptation for image denoising experiment

Encoder	Decoder
Conv(3 → 64, 3 × 3 kernel) +ReLU + MaxPool(2)	Linear(2 → 128)
Conv(64 → 128, 3 × 3 kernel) +ReLU + MaxPool(2)	Conv(128 → 64, 3 × 3 kernel) +ReLU + Upsample(2)
Conv(128 → 128, 3 × 3 kernel) +ReLU + MaxPool(2)	Conv(64 → 64, 4 × 4 kernel) +ReLU + Upsample(4)
Conv(128 → 128, 3 × 3 kernel) Linear(128 → 2)	Conv(64 → 3, 3 × 3 kernel)
Domain discriminator	
Linear(2 → 64) + ReLU	
Linear(64 → 64) + ReLU	
Linear(64 → 1)	
Generator (RW)	Discriminator (RW)
Linear(2 → 128)	Linear(2 → 128) + ReLU
Linear(128 → 128)	Linear(128 → 128) + ReLU
Linear(128 → 2)	Linear(128 → 1)
Hyperparameters	
Encoder learning rate	0.0002
Decoder learning rate	0.0002
Domain Discriminator learning rate	0.0002
Generator (RW) learning rate	0.0002
Discriminator (RW) learning rate	0.0002
π learning rate	0.0005
Batch size	128
Optimizer	Adam
Number of critic iters	5
Initial iters	5000
Weight clipping value	[−0.01, 0.01]
λ	1

A.3. Adversarial clustering

For adversarial clustering in imbalanced MNIST dataset (Section 5 of the main paper), the architectures and hyper-parameters used are given in Table 13.

A.4. Hypothesis testing

For hypothesis testing experiment (Section 6 of the main paper), the same model architectures and hyper-parameters as the MOG experiment (Table 8) was used.

B. Learning π

Computing normalized Wasserstein GAN requires optimizing \mathbf{G} , $\pi^{(1)}$ and $\pi^{(2)}$. $\pi^{(1)}$ and $\pi^{(2)}$ are k dimensional vectors in an simplex. Hence, the following constraints have to be satisfied while optimizing them:

$$\sum_i p_i^{(1)} = 1$$

$$\sum_i p_i^{(2)} = 1$$

To enforce this constraint in an end-to-end optimization, we

Table 13. Architectures and hyper-parameters: Mixture models on imbalanced-MNIST3 dataset

Generator	Discriminator
ConvTranspose(100 → 256, 4 × 4 kernel, stride 1) Batchnorm + ReLU	Spectralnorm(Conv(1 → 64, 4 × 4 kernel, stride 2)) LeakyReLU(0.2)
ConvTranspose(256 → 128, 4 × 4 kernel, stride 2) Batchnorm + ReLU	Spectralnorm(Conv(64 → 128, 4 × 4 kernel, stride 2)) LeakyReLU(0.2)
ConvTranspose(128 → 64, 4 × 4 kernel, stride 2) Batchnorm + ReLU	Spectralnorm(Conv(128 → 256, 4 × 4 kernel, stride 2)) LeakyReLU(0.2)
ConvTranspose(64 → 1, 4 × 4 kernel, stride 2) Tanh()	Spectralnorm(Conv(256 → 1, 4 × 4 kernel, stride 1))
Hyperparameters	
Discriminator learning rate	0.00005
Generator learning rate	0.0001
π learning rate	0.001
Batch size	64
Optimizer	RMSProp
Number of critic iters	5
Weight clip	[-0.01, 0.01]
λ_{reg}	0.01

use softmax function.

$$\begin{aligned}\pi^{(1)} &= \text{softmax}(\tilde{\pi}^{(1)}) \\ \pi^{(2)} &= \text{softmax}(\tilde{\pi}^{(2)})\end{aligned}$$

The new variables $\tilde{\pi}^{(1)}$ and $\tilde{\pi}^{(2)}$ become the optimization variables. The softmax function ensures that the mixture probabilities $\pi^{(1)}$ and $\pi^{(2)}$ lie in a simplex.

C. Additional results

C.1. CIFAR-10

We present results of training Normalized Wasserstein GAN on CIFAR-10 dataset. We use WGAN-GP (Gulrajani et al., 2017) with Resnet-based generator and discriminator models as our baseline method. The proposed NWGAN was trained with $k = 4$ modes using the same network architectures as the baseline. Sample generations produced by each mode of the NWGAN is shown in Figure 5. We observe that each generator model captures distinct variations of the entire dataset, thereby approximately disentangling different modes in input images. For quantitative evaluation, we compute inception scores for the baseline and the proposed NWGAN. The inception score for the baseline model is 7.56, whereas our model achieved an improved score of 7.89.

C.2. Domain adaptation under uniform mode proportions

In all experiments performed in the main paper, the source and the target domains varied in mode proportion. Our

Table 14. MNIST → MNIST-M settings

Config	3 modes	5 modes	10 modes
Classes	{1, 4, 8}	{0, 2, 4, 6, 8}	{0, 1, ..., 9}
Proportion of source samples	{0.63, 0.31, 0.06}	{0.33, 0.26, 0.2, 0.13, 0.06}	{0.15, 0.15, 0.15, 0.12, 0.12, 0.11, 0.05, 0.05, 0.05, 0.05}
Proportion of target samples	{0.06, 0.31, 0.63}	{0.06, 0.13, 0.2, 0.26, 0.33}	{0.05, 0.05, 0.05, 0.05, 0.11, 0.12, 0.12, 0.15, 0.15, 0.15}

experiments suggest that minimizing NW distance helps resolve the negative transfer witnessed while minimizing Wasserstein (or) adversarial distance on such data distributions. But, what happens when the source and the target distributions have uniform mode proportion? In fact, this is the setting considered in most of the previous unsupervised domain adaptation papers (Ganin & Lempitsky, 2015; Tzeng et al., 2017; Long et al., 2016; Shen et al., 2018), the one where the classical distance measures have shown to be successful. We intend to study the behaviour of NW distance in this setting.

Two adaptation experiments are considered - (1) MNIST → MNIST-M, each dataset having 10 classes with uniform mode proportion, and (2) Synthetic to real adaptation on VISDA: source and target domains contain 3 classes - *aeroplane*, *horse* and *truck* with uniform mode proportion. The results of performing adaptation using NW distance in comparison with classical distance measures are reported in Table 15 and 16. We observe that NW distance performs on par with the compared methods on both the datasets. This experiment demonstrates the effectiveness of NW distance on a range of settings – when the source and target datasets are balanced in mode proportions, NW becomes equivalent to Wasserstein distance and minimizing it is no worse than



Figure 5. Sample generations produced by the proposed NWGAN trained on CIFAR-10 with $k = 4$ generator modes.

minimizing the classical distance measures. On the other hand, when mode proportions of source and target domains differ, NW distance renormalizes the mode proportions and effectively performs domain adaptation. This illustrates the usefulness of NW distance in domain adaptation problems.

Table 15. Domain adaptation on mode-balanced datasets: MNIST \rightarrow MNIST-M. Average classification accuracies averaged over 5 runs are reported

Method	Classification accuracy (in %)
Source only	60.22
DANN	85.24
Wasserstein	83.47
Normalized Wasserstein	84.16

Table 16. Domain adaptation on mode-balanced datasets: VISDA. Average classification accuracies averaged over 5 runs are reported

Method	Classification accuracy (in %)
Source only	63.24
DANN	84.71
Wasserstein	90.08
Normalized Wasserstein	90.72

C.3. Adversarial clustering: Quantitative metrics

- Cluster purity: Cluster purity measures the extent to which clusters are consistent i.e., if each cluster contains similar points or not. To compute the cluster purity, the cardinality of the majority class is computed for each cluster, and summed over and divided by the total number of samples.
- ARI - Adjusted Rand Index: The rand index computes the similarity measure between two clusters by considering all pairs of samples, and counting the pairs of samples having the same cluster in the ground-truth and predicted cluster assignments. Adjusted rand index makes sure that ARI score is in the range $(0, 1)$

- NMI - Normalized Mutual Information: NMI is the normalized version of the mutual information between the predicted and the ground truth cluster assignments.

C.4. Adversarial clustering of CIFAR+CelebA

In this section, we show the results of performing adversarial clustering on a mixture of CIFAR-10 and CelebA datasets. The same dataset presented in Section 3.2 of the main paper is used in this experiment (i.e) the dataset contains CIFAR-10 and CelebA samples in 1 : 2 mode proportion. NWGAN was trained with 2 modes - each employing Resnet based generator-discriminator architectures (same architectures and hyper-parameters used in Section 3.2 of main paper). Quantitative evaluation of our approach in comparison with $k - \text{means}$ is given in Table 17. We observe that our approach outperforms $k - \text{means}$ clustering. However, the clustering quality is poorer than the one obtained on imbalanced MNIST dataset. This is because the samples generated on MNIST dataset had much better quality than the one produced on CIFAR-10. So, as long as the underlying GAN model produces good generations, our adversarial clustering algorithm performs well.

Table 17. Performance of clustering algorithms on CIFAR+CelebA dataset

Method	Cluster Purity	NMI	ARI
k-means	0.667	0.038	0.049
Normalized Wasserstein	0.870	0.505	0.547